Pharm Res (2013) 30:2050–2062
DOI 10.1007/s11095-013-1058-8

RESEARCH PAPER

The Potential Efficacy of R8-Modified Paclitaxel-Loaded Liposomes on Pulmonary Arterial Hypertension

Yujia Yin • Xindan Wu • Zhangya Yang • Jian Zhao • Xiaoshuang Wang • Qianyu Zhang • Mingqing Yuan • Liang Xie • Hanmin Liu • Qin He

Received: 11 December 2012 / Accepted: 10 April 2013 / Published online: 12 June 2013

ABSTRACT

Purpose In this paper, a novel liposomal formulation of paclitaxel modified with octaarginine (R8) was fabricated and the therapeutic efficacy of it on pulmonary arterial hypertension was evaluated.

Methods Octaarginine-modified stealth liposomes loaded with PTX (R8-PTX-LIP) were prepared and characterized. Vector cytoxicity and anti-proliferation ability of different formulations on primary cultured VSMCs were determined with MTT assay. The uptake capacity of VSMCs on different formulations were evaluated by flow cytometry, and the influences on cytoskeletons of liposomes were investigated by cytoskeleton staining with rhodamine-phalloidin. The biodistribution of liposomes were imaged by a CCD camera using a near-infrared fluorophore DiD. The therapeutic efficacy of different PTX-formulations of PAH was evaluated by hemodynamic measurement, right ventricular hypertrophic parameters and vessel diameters.

Results The cellular uptake of R8 modified liposomes (R8-LIP) was improved noticeably compared with other groups. All liposomes did not exert cytotoxicity on VSMCs in 24 h. R8-PTX-LIP exhibited the strongest inhibitory effect on the proliferation of VSMCs among all the formulations ($p < 0.001$). R8-PTX-LIP could reverse the phenotype transformation, and inhibit cell migration. mPAP, (RV/LV+S) and the wall thickness of small distal pulmonary arteries of rats treated with R8-PTX-LIP were significantly lower than those from other groups ($p < 0.001$).

Conclusions In conclusion, the drug delivery system of R8-modified paclitaxel-loaded liposomes we established showed pronounced inhibitory effect over VSMCs proliferation and cytoskeleton formation *in vitro*, a stronger pulmonary delivery ability *in vivo*, and was effective on PAH, showing the potential for pulmonary drug delivery system for PAH treatment.

KEY WORDS octaarginine · paclitaxel · pulmonary arterial hypertension · vascular smooth muscle cells

ABBREVIATIONS

Chol	Cholesterol
CLIP	Conventional liposomes
FBS	Fetal bovine serum
LV+S	The left ventricular and septum
MCT	Monocrotaline
mPAP	Mean pulmonary arterial pressure
NIR	Near-infrared

Y. Yin • X. Wang • L. Xie • H. Liu (✉)
The Pulmonary Vascular Remodeling Research Unit
Department of Pediatric, West China Second University Hospital
Sichuan University, No. 20, Section 3, RenminNanLu Road
Chengdu, Sichuan 610041, People's Republic of China
e-mail: myuxuan@163.net

Y. Yin • Q. Zhang • M. Yuan • Q. He
Key Laboratory of Drug Targeting and Drug Delivery Systems
West China School of Pharmacy Sichuan University
Chengdu, Sichuan 610041, People's Republic of China

X. Wang • L. Xie • H. Liu
Key Laboratory of Obstetric & Gynecologic and Pediatric Diseases and Birth Defects of Ministry of Education
West China Second University Hospital, Sichuan University
Chengdu, Sichuan 610041, People's Republic of China

Q. He
Key Laboratory of Smart Drug Delivery, Ministry of Education & PLA
Fudan University Shanghai 201203, People's Republic of China

X. Wu • Z. Yang • J. Zhao
Luzhou Medical College
Luzhou City, Sichuan 646000, People's Republic of China

Q. He (✉)
West China School of Pharmacy, Sichuan University No. 17, Block 3
Southern Renmin Road
Chengdu, Sichuan 610041, People's Republic of China
e-mail: qinhe317@126.com

PAH	Pulmonary arterial hypertension
PAP	Pulmonary artery pressure
PEG-LIP	PEG modified liposomes
PEG-PTX-LIP	Sterically stabilized paclitaxel loaded liposomes
PTX	Paclitaxel
PVR	Pulmonary vascular resistance
R8	Octaarginine
R8-LIP	R8 modified liposomes
R8-PTX-LIP	R8-modified paclitaxel-loaded liposomes
RV	The right ventricular
RV/(LV+S)	Ratio of Right Ventricular Weight to Left Ventricular Plus Septal Weight
TLC	Thin layer chromatography
VSMCs	Vascular smooth muscle cells
WT%	The percent medial wall thickness

INTRODUCTION

Pulmonary arterial hypertension (PAH) is a common clinical disorder in cardiovascular field. It is a syndrome resulting from restricted flow through the pulmonary arteries, which leads to pathological increases in pulmonary artery pressure (PAP) and pulmonary vascular resistance (PVR), and ultimately right heart failure or death (1). Multiple pathogenic pathways have been implicated in the development of PAH, and the evidences from pathology have proved that pulmonary vascular remodeling is one of the basic pathological characteristics of this disorder (2). The proliferation and migration of vascular smooth muscle cells (VSMCs) could be the core link of pulmonary vascular remodeling (3). Therefore, how to delay or reverse the pulmonary vascular remodeling is the key point of therapeutic strategy on PAH, and VSMCs are considered to be an important target because of their critical role in the developing of PAH.

Paclitaxel (PTX) has shown significant anti-tumor activity against several tumors such as breast cancer, advanced ovarian carcinoma, lung cancer, head and neck carcinoma, and acute leukemias when administered systemically (4). In addition, PTX also has been used in drug-eluting stents to prevent restenosis in the field of interventional cardiology. PTX was found to interfere with VSMCs' migration and proliferation at nanomolar levels *in vitro* (5). The target for PTX appears to be microtubules, which are important members of the cytoskeleton and play critical roles in several cellular functions, such as cell division, cell migration, and the maintenance of cell shape (6). PTX disrupts the mitosis and inhibits cell proliferation by steadying polymerized microtubules and enhancing microtubule assembly (7). Cell replication is blocked predominantly in the G_0/G_1 and G_2/M phases of the cell cycle. PTX is highly lipophilic, which enables it to penetrate cell membrane easily and hence promotes rapid cellular uptake. Therefore, PTX had been identified as a promising antiproliferative agent and could be a promising candidate in therapeutic strategy on PAH. However, due to its low solubility in water, it is usually administered dissolved in Cremophor EL and ethanol, which are associated with vehicle toxicity and cause serious side effects (8). Therefore, it is quite necessary to develop an effective and safe delivery system for PTX.

Liposomes have been widely used in pulmonary drug delivery for multiple applications including solubilization, sustained release, cellular and intracellular targeting, and minimization of toxicity (9). Drug loaded liposomes injected *via* tail vein are captured by reticuloendothelial system, vascular endothelial cells, and VSMCs in deep lung during the pulmonary circulation. Modifying the surface of liposomes with ligands would further enhance the uptake of the carrier system by the lung cells, increase the drug concentration in the lungs while reduce the drug concentration in the system, and finally reduce side effects. Liposome is considered as a good candidate for pulmonary drug delivery owing to its characteristics, such as ability to load hydrophilic and hydrophobic drugs, superficial modified possibility, chemical similarity with lung surfactant, good compatibility and low toxicity.

To improve the cellular uptake of liposomes, modifications on the surface were usually carried out. Octaarginine (R8) is a member of cell penetrating peptides, consisting of eight arginines (10,11). Recent studies have shown that, modification of liposomes with R8 could enhance the cellular uptake (12–14).

In this study, a novel liposomal formulation for pulmonary drug delivery was fabricated and characterized. The R8-modified liposomes were designed to load PTX in the phospholipid bilayers and to enhance cellular uptake of this drug, with its inhibitory effect on the proliferation of VSMCs investigated. We evaluated the biodistribution in lung and the treatment efficacy of this novel drug delivery system on PAH, and all the results clearly suggested that the liposomal formulation could be a promising candidate for treating this disease.

MATERIALS AND METHODS

Materials

1,2-distearoyl-sn-glycero-3-phosphoethanolamine-N-[maleimide (polyethylene glycol)-2000] (ammonium salt) (DSPE-PEG_{2000}-Mal), 1,2-distearoyl-sn-glycero-3-phosphoethanolamine-N-[methoxy (polyethylene glycol)-2000] (ammonium salt)(DSPE-PEG_{2000}), and FITC-PE were purchased from Avanti Polar Lipids, Inc (Alabaster, AL,

USA). MTT, SPC and Cholesterol (Chol) were purchased from Kelong Chemical Reagent Company (Chengdu, China). Octaarginine (R8) was synthesized by Chengdu Kai Jie Bio-pharmaceutical Co. Ltd. (Chengdu, China). Paclitaxel (PTX) was purchased from AP Pharmaceutical Co., Ltd (Chongqing, China). DID was obtained from Biotium (Hayward, CA, USA). Rhodamine-labeled phalloidin, PDGF-BB, Monocrotaline (MCT) were purchased from Sigma-Aldrich (St Louis, MO, USA). Methanol, chloroform, and the other reagents were all analytical grade.

Animals

Male Sprague–Dawley rats were purchased from West China animal center of Sichuan University (Sichuan, China). All animal procedures for this study were approved by the Experiment Animal Administrative Committee of Sichuan University.

Synthesis of R8 Peptide Conjugated PEG_{2000}-Lipid (R8-PEG_{2000}-Lipid)

The material was synthesized as previously described with some changes (15). R8 and DSPE-PEG_{2000}-Mal (molar ratio: 1.5:1) were mixed in chloroform/methanol (v/v=2:1) at room temperature with gentle stirring for 48 h. Triethylamine was employed as a catalyst. Thin layer chromatography (TLC) was applied to monitor the reaction process. When DSPE-PEG_{2000}-Mal disappeared on TLC, the mixture was evaporated under vacuum, the residue was re-dissolved with chloroform, the insoluble material was filtered, and the supernatant (DSPE-PEG_{2000}-R8) was evaporated again under vacuum and stored at −20°C.

Conjugation of the peptide to DSPE-PEG_{2000}-Mal was confirmed by determining the molecular weight of the resulting DSPE-PEG_{2000}-R8.

Preparation and Characterization of Liposomes

Lipid compositions of the prepared liposomes were as follows: (1) R8 modified liposomes (R8-LIP), SPC/Chol/DSPE-PEG_{2000}/DSPE-PEG_{2000}-R8 (molar ratio 59:33:3:5); (2) PEG modified liposomes (PEG-LIP), SPC/Chol/DSPE-PEG_{2000} (molar ratio 59:33:8); (3) conventional liposomes (CLIP), SPC/Chol (molar ratio 67:33). To label the lipid phase, FITC-PE or DID were incorporated at 5 mol% of total lipid. Liposomes were formed by thin film-ultrasonic method. In brief, a lipid film was produced by rotary evaporation of all lipids in chloroform. The films were left under vacuum for 2 h. Hydration buffer, PBS pH 7.4 was then added to produce a concentration of 10 μmol/3 ml of lipid. The lipid suspensions were intermittently sonicated with a probe sonicator at 80 W for 2 min. Paclitaxel and lipid ingredients, at a drug-to-lipid molar ratio of 1:40, were dissolved in chloroform to prepare drug-loaded liposomes following the steps described above. The free drug was removed using a Sephadex-G50 column, and the pellets were collected. Samples were diluted with pure water, and the mean diameters and zeta-potentials of liposomes were measured by Malvern Zetasizer Nano ZS90 (Malvern Instruments Ltd., UK).

The envelopment efficiency of liposomes was determined by HPLC (1200 Series, Agilent, USA) as follows. Liposome suspensions before or after the passage of Sephadex G-50 column were collected respectively as sample A and sample B. 1 ml of each samples was dissolved by adding 1 ml of methanol. After centrifugation, 20 μl of each solution was injected into a C_{18} column with a mobile phase of acetonitrile-water (55:45). The envelopment efficiency of liposomes was measured at 227 nm by detecting the UV adsorption of paclitaxel.

Primary Culture of VSMC and Immunohistochemical Identification

Vascular smooth muscle cells (VSMCs) were obtained by primary cell culture. Male Sprague–Dawley (SD) rats, approximately weighing from 100 g to 140 g (West China animal center of Sichuan University) were sacrificed, and pulmonary artery was taken out immediately. Connective tissue, tunica intima and tunica adventitia of the tissue were peeled under the asepsis condition, and then the tissue was cut into pieces of 1 ~ 2 mm^3. When tissue blocks clung to cell culture flask after 1 h, Dulbecco's modified Eagle's medium (Gibco, USA) containing 20% fetal bovine serum (FBS, Gibco, USA) was added. Cells would migrate from blocks to the bottom of bottles at 37°C in a humidified incubator with 5% CO_2 in 4 ~ 6 days. Trypsin (HyClone, USA) was used in the cell passaging. Experiments were performed with the cells from third to sixth generations.

VSMCs were purified and identificated by immunocytochemistry. VSMCs were fixed with 4% paraformaldehyde, and then incubated with primary antibody (Anti-alpha smooth muscle Actin antibody) at 37°C for 1 h. The secondary antibody was Peroxidase-conjugated affinipure goat anti-rabbit IgG. Cells were counterstained with hematoxylin. Sections were examined by microscope, and positive cells were counted within the same field of vision to evaluate the cell purity.

Quantification of Cell Uptake of Liposomes by VSMC

To compare the cellular uptake of R8-LIP, PEG-LIP and CLIP, 5×10^5 cells/well VSMC cells were seeded on a 6-well plate. The culture medium was refreshed, and then,

R8-LIP, PEG-LIP and CLIP labeled with FITC-PE were respectively added and incubated for 2 h at 37°C. At the end of the incubation, the culture medium was removed, and the cells were washed with ice-cold PBS (pH 7.4) supplemented with heparin for three times. Then, the cells were trypsinized and collected. Subsequently, the cells were washed twice by centrifugation (2,500 rpm, 4°C, 8 min) and were suspended in 1 ml of heparin-PBS. Finally, cells were suspended in 0.5 ml of PBS and were analyzed by a flow cytometer.

Cytotoxicity and Anti-Proliferative Activity Against VSMCs

It has been reported that the anti-proliferation of PTX on VSMCs is dependent on concentration, and the optimal concentration is at $10 \sim 100$ nmol/L^{-1} (5,16). According to the EE%, the lipid amounts of R8-LIP and PEG-LIP required for loading PTX 5 nmol/L, 25 nmol/L, 50 nmol/L, 75 nmol/L, 100 nmol/L were calculated, and denoted by R8-LIP-5, R8-LIP-25, R8-LIP-50, R8- LIP-75, R8-LIP-100, PEG-LIP-5, PEG-LIP-25, PEG-LIP-50, PEG-LIP-75, PEG-LIP-100. Cytotoxicity of these formulations was evaluated with MTT assay.

VSMCs were incubated in 96-well plates at a density of 1×10^5 cells/well. The adhering VSMCs were starved for 24 h with serum-free media. VSMCs in three wells cultured without liposomes were designed as the control, and other wells were divided into ten groups described above. All of the groups were cultured for a further 24 h with different formulations. MTT at a concentration of 5 mg/ml was added to each well cultured for 4 h, and then the media was replaced by DMSO (150 μl) in wells incubated for 10 min. Absorbance at 490 nm was measured with Microplate Reader. The percentage survival was calculated by the following formula. Each assay was repeated in triplicates.

$$\text{percentage survival} = \frac{[\text{Abs}]_{\text{sample}}}{[\text{Abs}]_{\text{control}}} \times 100\%$$

Anti-proliferative activity was also evaluated with MTT assay. VSMCs were incubated in 96-well plates at a density of 1×10^5 cells/well. The adhering VSMCs were starved for 24 h with serum-free media. Then, the wells were divided into five groups. All of the groups were cultured for a further 48 h with the presence of 20 ng/ml PDGF-BB, and four of them were treated respectively with R8-modified paclitaxel-loaded liposomes (R8-PTX-LIP), sterically stabilized paclitaxel loaded liposomes (PEG-PTX-LIP), free paclitaxel, and ethanol solvent at the same time, and one group only cultured with PDGF-BB was designed as the control. The concentration of paclitaxel administered in these groups was 100 nmol/ml. The following treatment was the same with the procedures described above, and the percentage inhibition was calculated by the following formula: percentage inhibition $= \frac{[\text{Abs}]_{\text{control}} - [\text{Abs}]_{\text{sample}}}{[\text{Abs}]_{\text{control}}} \times 100\%$. Each assay was repeated in triplicates.

Cytoskeleton Staining with Rhodamine-Phalloidin

Cytoskeleton of VSMCs was stained with Rhodamine-Phalloidin as described (17). VSMCs were seeded on slides in six-well plates until≈80% confluence. After serum deprivation for 24 h, cells were incubated at 37°C for a further 24 h with the experimental medium containing the treatments including R8-PTX-LIP, PEG-PTX-LIP, R8-LIP, PEG-LIP, free paclitaxel and ethanol solvent in the presence of PDGF (10 ng/ml). The concentration of paclitaxel administered in these groups was 100 nmol/ml. In addition, another two groups with and without PDGF (10 ng/ml) respectively were designed, and were named PDGF-BB group, and blank group respectively. Cells were fixed and rendered permeable with 4% formaldehyde: 0.2% Triton X-100, washed with phosphate-buffered saline (containing 1% BSA), incubated with rhodamine-phalloidin for 30 min at 37°C, and examined by confocal microscopy.

Ex Vivo DID Dye Fluorescence Imaging

In order to evaluate the biodistribution of R8-LIP and PEG-LIP, lioposomes were labeled with DID, a near-infrared (NIR) fluorophore as previously described (18). For *in vivo* optical imaging, SD rats (100 g-150 g, West China animal center of Sichuan University) were injected intravenously *via* vena caudalis with DID-loaded liposomes. *Ex vivo* fluorescence imaging was performed at the time points including 5 min, 30 min, 1 h, 2 h, 4 h, 12 h and 24 h after probe injection. The animals were sacrificed by perfusion of sodium chloride in the heart, and were fixed in 4% paraformaldehyde. The whole lung were removed and placed into a whole-mouse imaging system. As DID fluorescent tag was used to localize the liposomes, the 644 nm excitation filter and the 665 nm emission filter were selected. Images were captured by the CCD camera embedded in the imaging system (Quick View 3000, Bio-Real, AUSTRIA).

Evaluations of the *In Vivo* Therapeutic Efficacy

The experimental protocols and treatments were operated as previously reported (19). All experiments were approved by the Animal Policy and Welfare Committee of the Sichuan University. Sixty adult male Sprague–Dawley rats (300 g$\sim$350 g, obtained from West China animal center of Sichuan University) were divided into 6 groups randomly,

ie, normal group, sham operation group, model group, R8-LIP-PTX group, PEG-PTX -LIP group, and free paclitaxel group.

MCT was dissolved in 0.5 mol/L HCl and then adjusted to pH 7.4 with 0.5 mol/L NaOH solution. Rats were housed with a 12/12-hour light/dark cycle and given water and standard rat diet *ad libitum*.

All the groups except the normal group and the sham operation group were suffered pneumonectomy plus MCT injection. On the 1st day, rats were injected atropine sulfate (50 μg/kg) subcutaneously in the left hindlimb and anesthetized by an intraperitoneal injection with 10% chloral hydrate (400 mg/kg). Then, left pneumonectomy was performed as described (19). On the 7th day, rats were injected in the nape with monocrotaline (MCT) (60 mg/kg) subcutaneously. The sham group suffered every step above but left pneumonectomy plus MCT. On the 4th week, drug intervention was performed by injecting intravenously *via* vena caudalis according to different groups, ie, R8-PTX-LIP group, PEG-PTX-LIP group, free paclitaxel group and normal group which were treated with 0.9% saline. The sham group and model group were treated with nothing. Paclitaxel (2 mg/kg) were administered to rats (16).

As for the hemodynamic measurement, 1 week after the administration, all rats were injected tropine sulfate (50 μg/kg) and anesthetized with 10% chloral hydrate. The experimental protocols were performed as previously described (20). The right jugular vein was separated, and cuted with a surgical scissor. A polyethylene catheter connected with a pressure transducer (BIOPAC) was inserted into the vein and passed through the right ventricle into the pulmonary artery to measure mean pulmonary arterial pressure (mPAP). The intravascular location of the catheter tip was monitored by pressure tracing.

To evaluate the right ventricular hypertrophy of rats, the RV/(LV+S) was measured. After hemodynamic measurement, the rats were sacrificed humanly by cervical dislocation, and hearts and lungs were harvested. The right ventricular (RV) wall was freed from the left ventricular and septum (LV+S), and dried with absorbent paper. Weight of the two was measured separately. Then, RV/(LV+S) was calculated.

The right lungs were flushed with 0.9% saline infused *via* the pulmonary artery, fixed with 10% formalin *via* the airways, and embedded in paraffin for further experiments. Tissue blocks were routinely processed into 4 μm paraffin sections, and stained with hematoxylin-eosin for light microscopy.

Vessel diameters of at least 20 pulmonary arterioles (<200 μm) were determined at ~400 magnifications. The external diameter and medial wall thickness were measured using a calibrated eyepiece micrometer. The percent of medial wall thickness (WT%) of each artery was calculated by using the following formula as previously described (21,22).

$$\mathrm{WT\%} = 2 \times \frac{\text{Medial wall thickness}}{\text{External diameter}} \times 100\%$$

Statistical Analysis

The statistical significance of differences between groups was evaluated by one-way analysis of variance (ANOVA), followed by Bartlett's test formultiple comparisons. A P value <0.05 was considered as statistically significant.

RESULTS

Characterization of the Liposomes

TOF MS ES+ confirmed the formation of DSPE-PEG_{2000}-R8 (Mw calculated=4176, Mw observed=4255). Observed value of molecular weight was very close to the calculated value of molecular weight, so we determined that the product was DSPE-PEG_{2000}-R8.

In this study, CLIP and PEG-LIP were control groups without R8-modification. Transmission electron microscopy of R8-LIP exhibited uniform spherical appearance, demonstrating the successful formation of the liposomes (Fig. 1). As shown in Table I, the average diameters of the three types of liposomes were less than 150 nm, and the PDI were less than 0.3. PTX loaded liposomes had an increased size, and R8-PTX-LIP increased to (156±2) nm, with no significant change in PDI. The charge distributed around the liposomes vesicles were negatively charged, and R8-LIP possessed slightly negative charge. The envelopment efficiencies of R8-PTX-LIP and PEG-PTX-LIP were all over 80%.

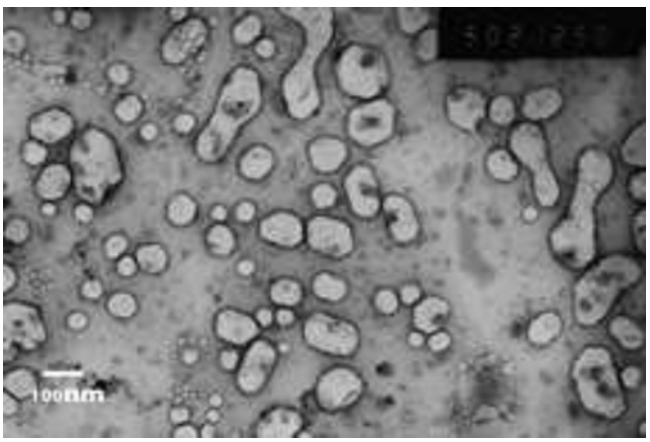

Fig. 1 Transmission electron microscopy of R8-LIP (×50,000).

Table I The Average Size and Zeta-Potential of Different Liposomes ($n = 3$)

	Average size (nm)	Polydispersity index (PDI)	zeta-potential (mV)
R8-LIP	128±7.5	0.25±0.016	−2.57±0.48
PEG-LIP	108±4.8	0.28±0.013	−4.65±0.41
CLIP	130±3.5	0.23±0.025	−30.11±1.13

VSMCs Immunohistochemical Identification

Immunohistochemistry showed that the majority of cells in Fig. 2 were stained positively, and the cytoplasm was brown. Microscopic counts of VSMCs showed that the purity was greater than 90%.

Quantification of Cellular Uptake of Liposomes by Flow Cytometric Analysis

After 2 h of incubation, the fluorescence values of VSMCs were measured by flow cytometer. Results showed that the fluorescence values in groups were significantly different as follows: R8-LIP group > CLIP group > PEG-LIP group (Fig. 3). Among all the groups, the internalization of liposomes modified with R8 was the most evident. The fluorescence value of R8-LIP group was 10 times and 6 times higher compared with those of PEG-LIP group and CLIP group respectively. We concluded that the cellular uptake of R8-LIP was improved noticeably by R8 modification compared with unmodified PEG-LIP and CLIP.

The curve represent (from left to right): blank, PEG-LIP group, CLIP-group, and R8-LIP group.

Cytotoxicity and Anti-Proliferative Effects against VSMCs

Cytotoxicity of liposomes was evaluated by MTT. Data (in Fig. 4) showed that all liposomes did not exhibit cytotoxicity

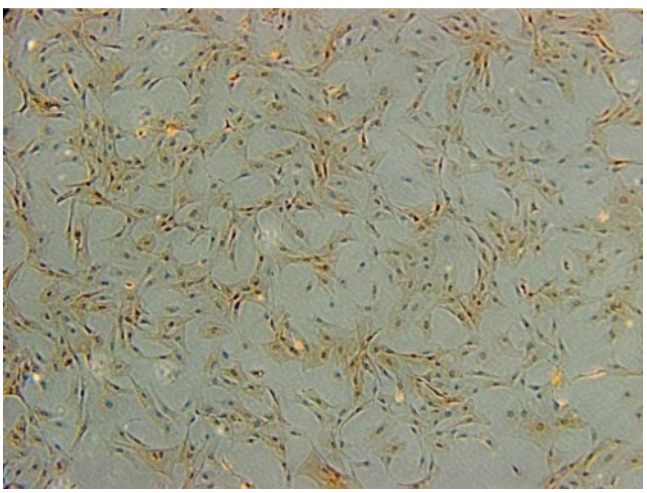

Fig. 2 Immunohistochemical identification of VSMCs.

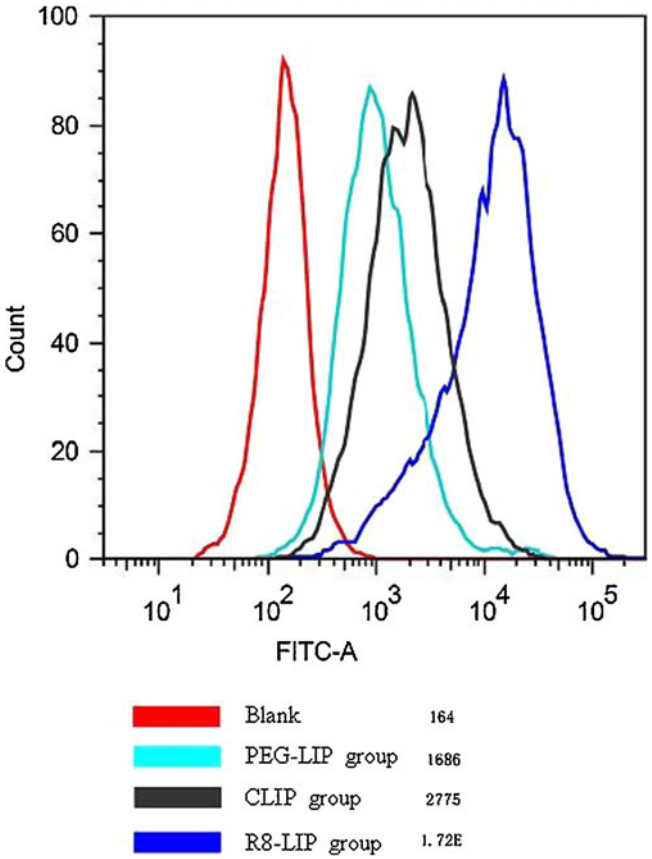

Fig. 3 Quantitative evaluation of different groups uptake by VSMCs.

on VSMCs in 24 h. In our study, the vehicles were safe for further *in vitro* and *in vivo* studies.

Figure 5 represented the anti-proliferative effect of each formulation on VSMCs. The results from MTT assay showed that the R8-PTX-LIP exhibited the strongest inhibitory effect on the proliferation of VSMCs among all formulations. The percentages inhibition of R8-PTX-LIP group, PEG-PTX-LIP group, free paclitaxel group, and ethanol solvent group were 64%, 36%, 29%, 10%, respectively. The percentage inhibition of R8-PTX-LIP group indicated that the anti-proliferative effect of the drug-loaded liposomes was markedly elevated by the modification with R8.

Effects on Cytoskeleton From Formulations

The assemble of F-actin in VSMCs treated with different liposomal preparations was observed by confocal microscopy. PDGF-BB induced the phenotype of VSMCs to transform from contractile type to synthetic type, which leading to proliferation and migration (23–26).To achieve cell migration, the amount of F-actin increased, and F-actin assembled stress fibers massively. As shown in Fig. 6c, intensive fluorescence represented that PDGF-BB (10 ng/ml) stimulated the expression of F-actin significantly, and the stress fibers consisting of F-actin ran through the cell long axis in dense bundles. Other groups except blank group, free paclitaxel group and R8-PTX-LIP

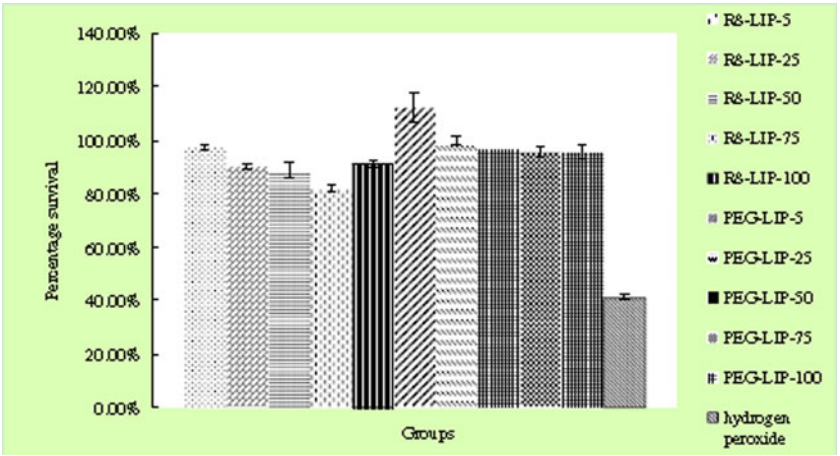

Fig. 4 The cytotoxicity of liposomes on VSMCs.

group shared the similar characteristics with PDGF-BB group. The expression of F-actin in free paclitaxel and R8-PTX-LIP group decreased evidently compared with others, and R8-PTX-LIP showed the strongest effect on F-actin. The stress fibers consisting of F-actin enabled cell motion; thus the alteration of cytoskeleton property means preventing cell migration. The observation of VSMCs phenotype showed that only the cells treated with R8-PTX-LIP obviously represented a elongated and spindle-shaped as contractile VSMCs. The cell shapes of blank group and PTX group were more regular than those of other groups except R8-PTX-LIP group. Treating with PTX alone did not achieve the level of phenotype transformation as R8-PTX-LIP did. The cells of other groups except the three groups including blank group, PDGF-BB group, and PTX group were typically synthetic VSMCs, which were irregular, less elongated and cobblestone morphology. This result showed that R8-PTX-LIP could reverse the phenotype transformation through the influence on cytoskeleton.

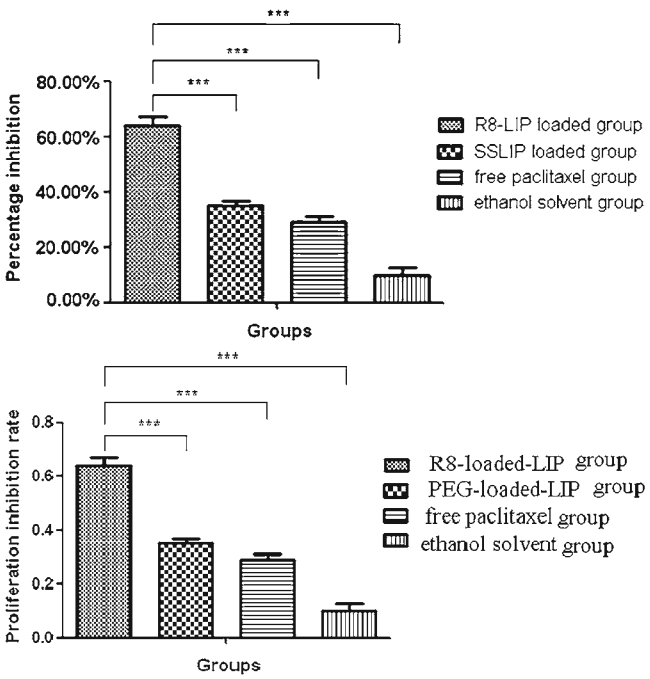

Fig. 5 Anti-proliferative effect by directly applying each formulation for 48 h ($n=5$, ***$p<0.001$).

Ex vivo Fluorescence Imaging

Nowadays, near-infrared (NIR) fluorescence imaging is considered as a potential tool for imaging (27,28). The NIR fluorescence imaging offers advantages such as nonradioactivity and high sensitivity compared with conventional techniques (15). At the wavelength of DID, light penetrated relatively deeply into the tissues. 5 min after the injection, a significantly stronger fluorescent signal was detected in lungs of R8-LIP group compared with those of PEG-LIP group and blank group. The fluorescent signal in R8-LIP group accumulated to a high level in 1 h, and maintained strong fluorescence for 24 h, whereas weak signals exhibited in the lungs of control animals treated with PEG-LIP during the same period of time (Fig. 7). R8 on the surface of R8-LIP might enhance the cellular uptake ability of this vehicle. However, in PEG-LIP group, PEG_{2000} with high density restricted the interaction between the PEG-LIP and cellular membrane. The stronger cellular uptake ability might be the reason why we found more fluorescence signals in R8-LIP group.

Evaluations of the *In Vivo* Therapeutic Efficacy

One week after the administration, mPAP of rats from different groups were measured and analyzed. mPAP were significantly decreased in R8-PTX-LIP group compared with those of model group, PEG-PTX-LIP group and free paclitaxel group ($p<0.001$). mPAP of R8-PTX-LIP group were 55%, 63% and 66% of model group, PEG-PTX-LIP group and free paclitaxel group respectively. mPAP of R8-PTX-LIP

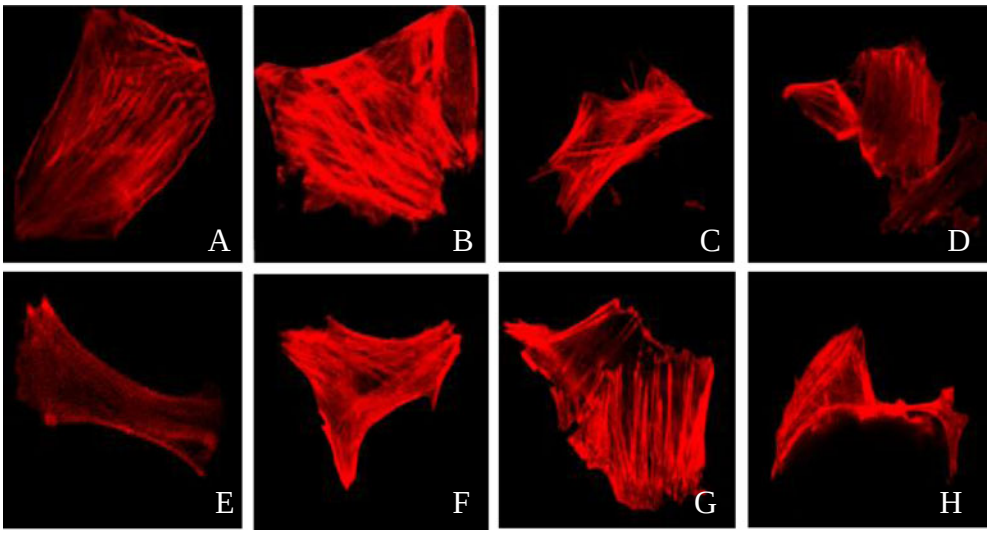

Fig. 6 Cytoskeletons of VSMCs with different treatments. (**a**) Blank; (**b**) ethanol solvent; (**c**) PDGF-BB; (**d**) free paclitaxel; (**e**) R8-PTX-LIP; (**f**) PEG-PTX-LIP; (**g**) R8-LIP; (**h**) PEG-LIP.

group was closed to normal group and sham group, but mPAP of PEG-PTX-LIP group and free paclitaxel group decreased slightly (Fig. 8). These data indicated that the paclitaxel-loaded liposomes modified with R8 prevented the increase of mPAP effectively in rats developing severe PAH.

To determine the RV/(LV+S) of different groups, hearts from different groups were harvested for the determination and comparison of RV/(LV+S). RV/(LV+S) of R8-PTX-LIP group was significantly lower than those of model group, PEG-PTX-LIP group and free paclitaxel group ($p<0.001$). RV/(LV+S) of R8-PTX-LIP group was decreased with 46%, 40% and 49% compared with those from model group, PEG-PTX-LIP group and free PTX group respectively. This parameter of R8-PTX-LIP group was closed to those of normal group and sham group (Fig. 9). These data indicated that the paclitaxel-loaded liposomes modified with R8 inhibited the increasing of RV/(LV+S) remarkably in rats developing severe PAH.

To evaluate the histological changes, we examined the pulmonary arteries of the lung specimens, and calculated the WT%. Evidence of rats developing severe PAH with the incrassate blood vessel wall was readily observed in histological sections prepared from model rats (in Fig. 10c), and pulmonary artery in model group was more thicker than those of normal group and sham group (in Fig. 10a, b). We also observed a significant decrease in wall thickness of pulmonary arteries of R8-PTX-LIP group (in Fig. 10d) compared with model group. To some extent, the treatment strategies with PEG-PTX-LIP or free PTX both exhibited an ability to inhibit the thickening of blood vessel wall (in Fig. 10e, f), but the therapeutic effects were not so significantly as R8-PTX-LIP group. WT% (in Fig. 11) showed the same trend.

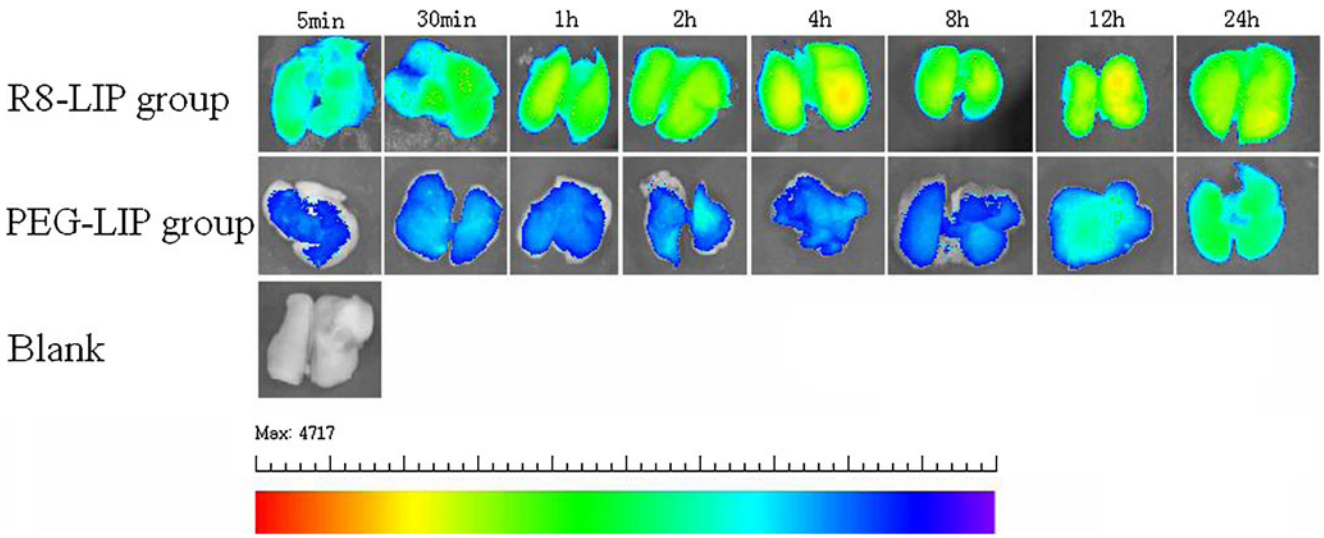

Fig. 7 *Ex vivo* imaging of lung given different DID-loaded liposomes *via* tail vein.

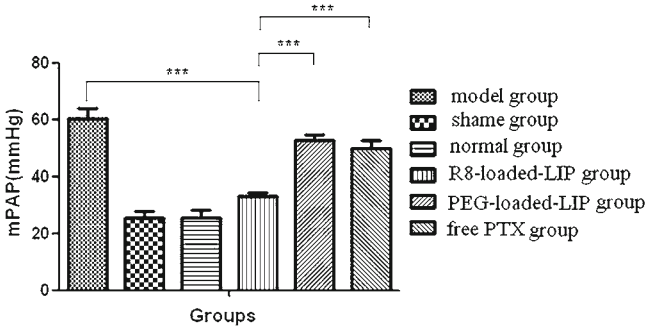

Fig. 8 Mean pulmonary artery pressure of rats ($n = 10$, ***$p < 0.001$).

Histopathological examinations of lung tissues revealed that, the walls of distal pulmonary arteries from R8-PTX-LIP rats were thin significantly compared with those of control groups.

DISCUSSION

PAH lead to an increase in pulmonary vascular resistance, right heart failure and death. The pathobiology of PAH involves a remodeling process in distal pulmonary arteries, as well as vasoconstriction and *in situ* thrombosis. VSMCs play important roles in the pulmonary vascular remodeling process, which made them to be a critical target in treating PAH.

PTX has proved itself an excellent anti-tumor agent against several tumors (4) *in vitro* study, *in vivo* study and for clinical application (31). In clinic, besides the anti-tumor activity, PTX has been incorporated in drug-eluting stents

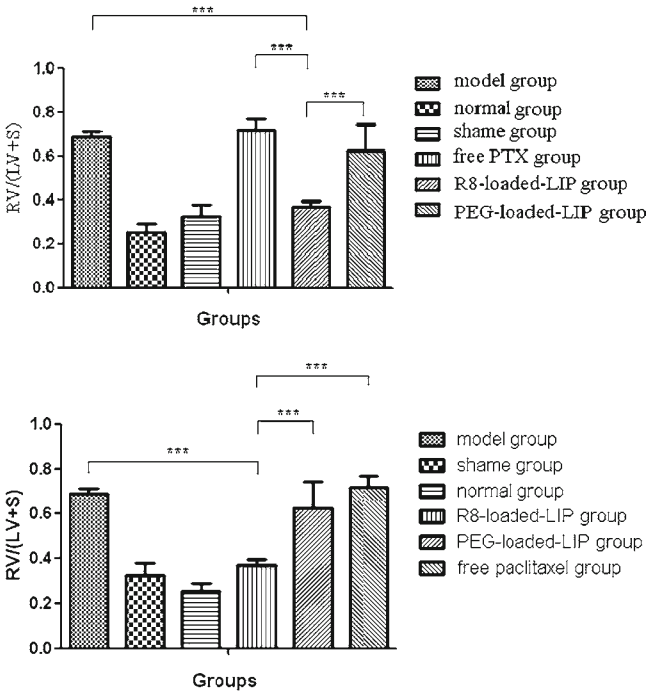

Fig. 9 RV/(LV+S) of different groups ($n = 10$, ***$p < 0.001$).

to prevent restenosis in the field of interventional cardiology (29). The mechanism of PTX action on cell is unique. The target of PTX is microtubules, which are important members of the cytoskeleton and play critical roles in several cellular functions, such as cell division, cell migration, and the maintenance of cell shape (6). PTX disrupts the mitosis and inhibits cell proliferation by steadying polymerized microtubules and enhancing microtubule assembly (7). Cell replication is blocked predominantly in the G0/G1 and G2/M phases of the cell cycle. In PAH, VSMCs perform an abnormal prolifercation which is the characteristics of tumor cells. Therefore, PAH seems like a"tumor"in cardiovascular field. Compared to the rather higher concentration applied in cancer therapy (Taxol® at the concentration of 6 mg/mL), it has been reported that the optimal concentration for the inhibition of proliferation of PTX on VSMCs is at 10 ~ 100 nmol/L (5,16). In this case, PTX can be a promising drug used in therapy of PAH considering the drug could inhibit VSMCs proliferation which is a core point in PAH process, and liposomes is the suitable carrier for PTX.

In this study, we developed a lung-targeted liposomal system modified with R8 to treat PAH. The nanomolar levels of PTX is reported to exhibit inhibition on VSMCs proliferation and migration (5), which is much lower than the dose used in tumor therapy, with little cytotoxicity on normal tissue cell. Since the liposomes modified with R8 loaded with paclitaxel for the treatment of PAH has not been reported elsewhere, the PTX-R8-LIP was designed and developed in our study.

Injected *via* tail vein, drug loaded liposomes are captured by reticuloendothelial system, vascular endothelial cells, and VSMCs in deep lung during the pulmonary circulation. Modifying the surface of liposomes with ligands would further enhance the uptake of the carrier system by the lung cells, increase the drug concentration in the lungs while reduce the drug concentration in the system, and finally reduce side effects. PTX has shown significant anti-tumor activity against several tumors such as breast cancer, advanced ovarian carcinoma, lung cancer, head and neck carcinoma, and acute leukemias when administered systemically (4). In clinic, besides the anti-tumor activity, PTX has been incorporated in drug-eluting stents to prevent restenosis in the field of interventional cardiology (29). Therefore, PTX can be a promising drug used in therapy of PAH considering the drug could inhibit VSMCs proliferation which is a key component in PAH pathological process, and liposomes is a suitable carrier for PTX. In this study, we developed a lung-targeted liposomal system modified with R8 to treat PAH.

The particle size is one of the most important formulation parameter for pulmonary drug delivery system. Larger particles about 4 ~ 7 μm incline to deposit in the airways, while smaller particles (1 ~ 3 μm) and those in submicron range (<1 μm) reach the lower airways and deeper lung (9).

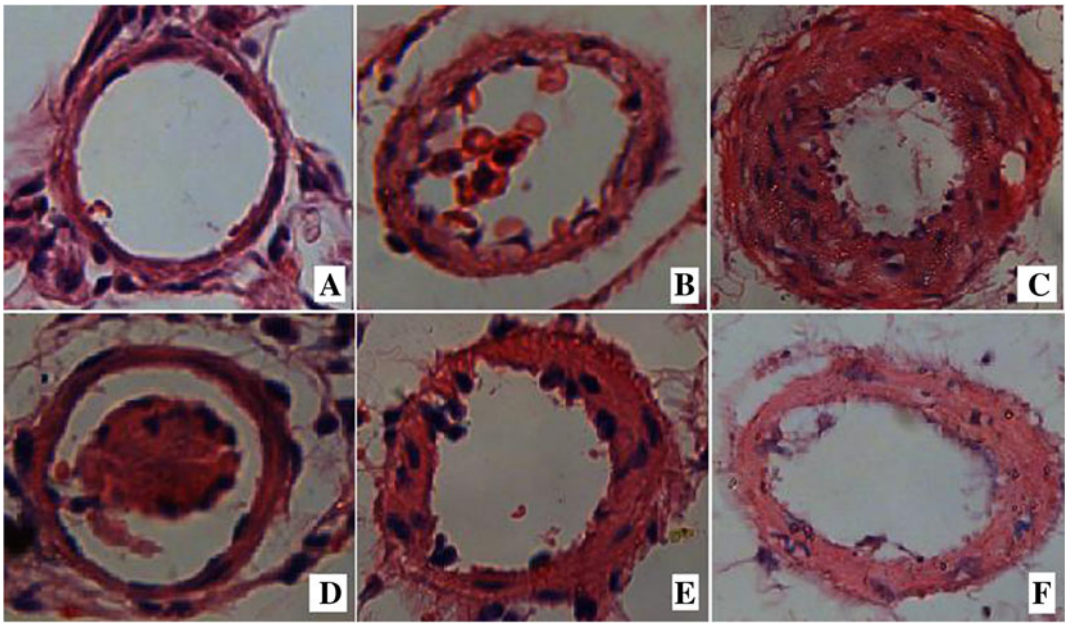

Fig. 10 Liposomes inhibits thickening in pulmonary arterioles (HE staining, magnification × 400). (**a**) Normal group; (**b**) Sham operation group; (**c**) Model group; (**d**) R8-PTX-LIP group; (**e**) PEG-PTX-LIP group; (**f**) Free PTX.

Therefore the proper size of liposomes influences the delivery activity in lung. In our study, the sizes of prepared liposomes were all about 100 ~ 200 nm, which provided a suitable particle size for pulmonary drug delivery. Liposomes at this range could reach deeper lung (9), and achieved a lung delivery ability. The size of PEG-LIP was smaller than that of R8-LIP, and the reason was that DSPE-PEG_{2000} in the liposomes brought about the stabilizing effect, which hindered the interactions between liposomes. The liposomes we prepared with size within 200 nm and PDI less than 0.3 were considered adequate for further *in vitro* and *in vivo* studies. As for the zeta-potentials, we've screened a series of formulations for this R8-modified liposomes with the content of R8 ranging from 1%–5%, but all of them exhibited zeta-potentials around −2.5 mV in pure water and −0.5 mV in PBS. Although not positive, the zeta potential of these R8-LIP (around −2.5 mV) were all slightly higher than the PEG-LIP (around −4.5 mV), indicating the possible influence of R8 on the surface charge of the liposomes. Zeta-potentials of liposomes were measured by Malvern Zetasizer Nano ZS90 (Malvern Instruments Ltd., UK) and it could be influenced by many factors such as pH and ionic strength. Different sources of lipid materials including the cholesterol and SPC might also render the zeta-potential different from previous observations. Though it presented slightly negative charge, R8-LIP possessed significant capability of cellular uptake comparing with unmodified liposomes as the previous observations.

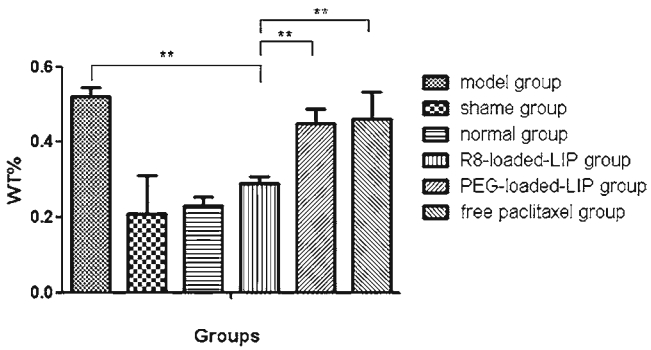

Fig. 11 WT% of pulmonary arterioles. ($n = 10$, $^{**}p < 0.01$).

CLIP performs an ability of cellular uptake with the charge on surface interaction with cellular membrane, but it is cleaned up quickly *in vivo*. To prolong the time of liposomes circulation *in vivo*, PEG_{2000} was applied to drug delivery systems. Liposomes modified with PEG_{2000} are frequently used in delayed or controlled formulation researches (30). Just as every coin has two sides, PEG-LIP obtained the poor cellular uptake at the same time, which might be due to the presence of PEG_{2000} with high density on the surface of liposomes. The existence of PEG_{2000} prevents the interaction between cell and PEG-LIP. So, in the vitro study, Fig. 3 showed that CLIP possessed better cellular uptake ability than PEG-LIP. R8-LIP is PEG-LIP modifying with R8, and this formulation owns the two dominances: long-circulating characteristics and excellent endocytosis.

PTX has proved itself an excellent anti-tumor agent *in vitro* study, *in vivo* study and for clinical application (31). The mechanism of PTX action on cell is unique. The target of PTX is microtubules, which are important members of the cytoskeleton and play critical roles in several cellular functions, such as cell division, cell migration, and the maintenance of cell shape (6). PTX disrupts the mitosis and inhibits cell

proliferation by steadying polymerized microtubules and enhancing microtubule assembly (7). Cell replication is blocked predominantly in the G_0/G_1 and G_2/M phases of the cell cycle. In PAH, VSMCs perform an abnormal prolifercation which is the characteristics of tumor cells. So, PAH seems like a "tumor" in cardiovascular field. Compared to the higher concentration applied in cancer therapy (Taxol® at the concentration of 6 mg/mL), it has been reported that the optimal concentration of PTX for the inhibition of proliferation of VSMCs is at 10~100 nmol/L (5,16) According to the mechanism of PTX, we supposed that PTX might prevent VSMCs proliferation in a low concentration (10~100 nmol/L) which was much lower than the dose used in tumor therapy, with little cytotoxicity on normal tissue cell. The nanomolar levels of PTX is reported to exhibit inhibition on VSMCs proliferation and migration (5), and PTX is considered to be a promising anti-proliferation agent. Base on its anti-proliferation ability, the application of PTX is designed and developed. PTX drug-eluting stents has been used in clinic (32–34). We loaded PTX in R8-LIP, and this PTX formulation inhibited the proliferation of VSMCs effectively. PEG-PTX-LIP and free PTX both forbade the cell proliferation, and the anti-proliferation ability of R8-PTX-LIP with the excellent endocytosis was much stronger. This result indicated that the vehicle we designed was effective *in vitro*.

Results from pathology reveal that complete vascular intima is very important for normal VSMCs phenotype-keeping. Injuries of vascellum allows VSMCs to get in touch with growth factors in blood, mainly PDGF. PDGF is a powerful mitogen and chemokines, which can significantly stimulate proliferation and migration in endothelial cells and VSMCs (36). The influence of PDGF on VSMCs has been demonstrated in animal experiments (35). In normal VSMCs, PDGF is hard to measure, but its expression significantly increased when vascellum was damaged or micro-environment changed (37). PDGF has three subtypes: PDGF-BB, PDGF-AA and PDGF-AB. PDGF-BB has been reported to induce VSMCs to transform from the contractile type to the synthetic type, accompanying with cell proliferation and migration (38). It is well known that PDGF-BB plays an important role in the development of atherosclerosis, restenosis after angioplasty, hypertension and other vascular remodeling (36). In our study, PDGF-BB was used to induce VSCMs proliferation and migration to simulate the abnormal VSMCs in PAH. Cell shapes in Fig. 6c showed that PDGF-BB induced the transformation of VSMCs into synthetic type which were less elongated and cobblestone morphology, but cells treated with R8-PTX-LIP were contractile VSMCs, which were elongated and spindle-shaped described previously(38). R8-PTX-LIP could reverse the phenotype transformation, and it might be effective on PAH.

The *ex vivo* NIR fluorescent imaging showed the qualitative biodistribution of liposomes in lungs, and revealed the lung delivery properties of each formulation more scientifically and directly. After injection, R8-LIP group and PEG-LIP group both showed fluorescent signal accumulation in lung, but the fluorescence intensity of each group was quite different. Compared with PEG-LIP group, R8-LIP group accumulated in lung at a very short time (5 min), and maintained strong fluorescence for 24 h. This results demonstrated that decoration of liposomes with R8 enhanced their cellular uptake, and R8-LIP was considered adequate for pulmonary drug delivery.

Left pneumonectomy plus MCT has been used extensively to demonstrate drug effectiveness in prevention and treatment of PAH. Hemodynamic factors have profound influences on blood vessels. mPAP had been tested in this animal model previously, and it increased to 50 mmHg (18). In our study, mPAP in model group was 60 mmHg, which was quite close to the reported value, indicating that PAH model we established was successful. The VSMCs proliferation caused pulmonary vascular remodeling, and blood pressure in PAH was abnormal finally. R8-PTX-LIP had better pulmonary drug delivery ability than PEG-PTX-LIP and free PTX, therefore, R8-PTX-LIP could accumulate in VSMCs more effectively. R8-PTX-LIP assisted PTX loading in the lipid bilayers to accumulate in VSMCs, and inhibited the cell proliferation. So mPAP of R8-PTX-LIP group decreased significantly in all treatment groups, and it was similar as normal group and sham group. Although PEG-PTX-LIP could accumulate in lung, this carrier had poor cellular uptake ability, and it did not have effective influence on VSMCs. PEG-PTX-LIP group showed a similar therapeutic effect with free PTX. Overall, mPAP showed that the R8-PTX-LIP could play a significant therapeutic effect on PAH.

With pulmonary artery pressure increased, the right heart load was increased at the same time. Right ventricular (RV) pressure overload causes right ventricular hypertrophy in PAH. Alterations in RV function always cause the associated cardiac dysfunction. Due to global neurohormonal adaptations and mechanical ventricular interaction, dysfunction in RV could affect left ventricular (LV) function as well. Rats model with monocrotaline (MCT)-induced RV hypertrophy were established to study LV function, RV function and their interaction. Results revealed that structural changes of the RV and LV resulted in depressed LV diastolic function during RV hypertrophy (39). It is important to take the thickening of RV into consideration, and RV/(LV+S) should be evaluated in PAH. RV/(LV+S) had been tested in this animal model previously, and it increased to 0.8 (18).In our study, RV/(LV+S) in model group was 0.7 ± 0.02, which was consistent with previous report.. Data from RV/(LV+S) revealed the same conclusion as above that R8-PTX-LIP could play a significant therapeutic effect on PAH in rats.

CONCLUSION

The drug delivery system of R8-modified paclitaxel-loaded liposomes we established showed pronounced inhibitory effects over VSMCs proliferation and cytoskeleton *in vitro*, a stronger pulmonary delivery ability *in vivo*, and was effective on PAH. Therefore PTX-R8-LIP proved itself a very potential pulmonary drug delivery system for PAH treatment.

ACKNOWLEDGMENTS AND DISCLOSURES

This research was supported by the National Natural and Science Foundation of China (No. 81072599), Program for Changjiang Scholars and Innovative Research Team in University (No. IRT0935) and the School of Pharmacy, Fudan University & The Open Project Program of Key Lab of Smart Drug Delivery, Ministry of Education & PLA, China.

REFERENCES

1. McLaughlin VV, Archer SL, Badesch DB, Barst RJ, Farber HW, Lindner JR, *et al.* ACCF/AHA 2009 expert consensus document on pulmonary hypertension. Circulation. 2009;119(16):2250–94.
2. Jeffery TK, Morrell NW. Molecular and cellular basis of vascular remodeling in pulmonary hypertension. Prog Cardiovasc Dis. 2002;45(3):173–202.
3. Mcgoon MD, Kane GC. Pulmonary hypertension: diagnosis and management. Mayo Clin Proc. 2009;84(2):191–207.
4. Kang BK, Chon SK, Kim SH, Jeong SY, Kim MS, Cho SH, *et al.* Controlled release of paclitaxel from microemulsion containing PLGA and evaluation of anti-tumor activity *in vitro* and *in vivo*. Int J Pharm. 2004;286:147–56.
5. Sollott SJ, Cheng L, Pauly RR, Jenkins GM, Monticone RE, Kuzuya M, *et al.* Taxol inhibits neointimal smooth muscle cell accumulation after angioplasty in the rat. J Clin Invest. 1995;95:1869–76.
6. Axel DI, Kunert W, Göggelmann C, Oberhoff M, Herdeg C, Küttner A, *et al.* Paclitaxel inhibits arterial smooth muscle cell proliferation and migration *in vitro* and *in vivo* using local drug delivery. Circulation. 1997;96:636–45.
7. Schiff PB, Fant J, Horwitz SB. Promotion of microtubule assembly *in vitro* by Taxol. Nature. 1979;277:665–7.
8. WeiSS RB, Donehower RC, Wiernik PH, Ohnuma T, Gralla RJ, Trump DL, *et al.* Hypersensitivity reactions from taxol. J Clin Oncol. 1990;8:1263–8.
9. Swaminathan J, Ehrhardt C. Controlled pulmonary drug delivery. New York: Springer; 2011.
10. Futaki S, Suzuki T, Ohashi W, Yagami T, Tanaka S, Ueda K, *et al.* Arginine-rich peptides. An abundant source of membrane-permeable peptides having potential as carriers for intracellular protein delivery. J Biol Chem. 2001;276:5836–40.
11. Suzuki T, Futaki S, Niwa M, Tanaka S, Ueda K, Sugiura Y. Possible existence of common internalization mechanisms among arginine-rich peptides. J Biol Chem. 2002;277:2437–43.
12. Futaki S, Ohashi W, Suzuki T, Niwa M, Tanaka S, Ueda K, *et al.* Stearylated arginine-rich peptides: a new class of transfection systems. Bioconjug Chem. 2001;12:1005–11.
13. Cryan SA, Devocelle M, Moran PJ, Hickey AJ, Kelly JG. Increased intracellular targeting to airway cells using octaarginine-coated liposomes: *in vitro* assessment of their suitability for inhalation. Mol Pharm. 2006;3(2):104–12.
14. Marty C, Meylan C, Schott H, Ballmer-Hofer K, Schwendener RA. Enhanced heparan sulfate proteoglycan-mediated uptake of cellpenetrating peptide-modified liposomes. Cell Mol Life Sci. 2004;61:1785–94.
15. Qin Y, Chen HL, Zhang QY, Wang XX, Yuan WW, Kuai R, *et al.* Liposome formulated with TAT-modified cholesterol for improving brain delivery and therapeutic efficacy on brain glioma in animals. Int J Pharm. 2011;420:304–12.
16. Kim DW, Kwon JS, Kim YG, Kim MS, Lee GS, Youn TJ, *et al.* Novel oral formulation of paclitaxel inhibits neointimal hyperplasia in a rat carotid artery injury model. Circulation. 2004;109:1558–63.
17. Yang XP, Thomas DP, Zhang XC, Culver BW, Alexander BM, Murdoch WJ, *et al.* Curcumin inhibits platelet-derived growth factor stimulated vascular smooth muscle cell function and injury-induced neointima formation. Arterioscler Thromb Vasc Biol. 2006;26:85–90.
18. Morille M, Montier T, Legras P, Carmoy N, Brodin P, Pitard B, *et al.* Long-circulating DNA lipid nanocapsules as new vector for passive tumor targeting. Biomaterials. 2010;31(2):321–9.
19. Okada K, Tanaka Y, Bernstein M, Zhang W, Patterson GA, Botney MD, *et al.* Pulmonary hemodynamics modify the rat pulmonary artery response to injury: a neointimal model of pulmonary hypertension. Am J Pathol. 1997;151(4):1019–25.
20. Mei YF, Jin H, Tian W, Wang H, Wang H, Zhao YP, *et al.* Urantide alleviates monocrotaline induced pulmonary arterial hypertension in Wistar rats. Pulm Pharmacol Ther. 2011;24:386–93.
21. Mathew R, Gloster ES, Sundararajan T, Thompson CI, Zeballos GA, Gewitz MH. Role of inhibition of nitric oxide production in monocrotaline-induced pulmonary hypertension. J Appl Physiol. 1997;82:1493–8.
22. Cowan KN, Heilbut A, Humpl T, Lam C, Ito S, Rabinovitch M. Complete reversal of fatal pulmonary hypertension in rats by a serine elastase inhibitor. Nat Med. 2000;6:698–702.
23. Kavanagh CA, Rochev YA, Gallagher WM, Dawson KA, Keenan AK. Local drug delivery in restenosis injury: thermoresponsive copolymers as potential drug delivery systems. Pharmacol Therapeut. 2004;102:1–15.
24. Kim TJ, Lim Y, Kim DW, Kwon JS, Son JH, Jin YR, *et al.* Epothilone D, a microtubule-stabilizing compound, inhibits neointimal hyperplasia after rat carotid artery injury by cell cycle arrest *via* regulation of G1-checkpoint proteins. Vasc Pharmacol. 2007;47:229–37.
25. Kenichi S, Takahisa M, Hiroko CH, Hori M, Ozaki H. Fluvastatin prevents vascular hyperplasia by inhibiting phenotype modulation and proliferation through extracellular signal regulated kinase 1 and 2 and p38 mitogenactivated protein kinase inactivation in organ-cultured artery. Arterioscler Thromb Vasc Biol. 2005;5(2):327–33.
26. Rensen SSM, Doevendans PAFM, Eys GJJM. Regulation and characteristics of vascular smooth muscle cell phenotypic diversity. Neth Heart J. 2007;:100–8. doi:10.1007/BF03085963.
27. Frangioni JV. *In vivo* near-infrared fluorescence imaging. Curr Opin Chem Biol. 2003;7:626–34.
28. Ntziachristos V, Bremer C, Issleder R. Fluorescence imaging with nearinfrared light: new technological advances that enable *in vivo* molecular imaging. Eur Radiol. 2003;13:195–208.
29. Wessely R, Schömig A, Kastrati A. Sirolimus and paclitaxel on polymer-based drug-eluting stents. J Am Coll Cardiol. 2006;47(No. 4).

30. Lei F, Fan W, Li XK, Wang S, Hai L, Wu Y, *et al.* Design, synthesis and preliminary bioevaluation of glucose–cholesterol derivatives as ligands for brain targeting liposomes. Chin Chem Lett. 2011;22(7):831–4.
31. Nativ O, Aronson M, Medalia O, Moldavsky T, Sabo E, Ringe I, *et al.* Anti-neoplastic activity of paclitaxel on experimental superficial bladder cancer: *in vivo* and *in vitro* studies. Int J Cancer. 1997;70:297–301.
32. Lao LL, Venkatraman SS. Adjustable paclitaxel release kinetics and its efficacy to inhibit smooth muscle cells proliferation. J Control Release. 2008;7(130):9–14.
33. Kastrati A, Dibra A, Eberle S, Mehilli J, Lezo JS, Goy JJ, *et al.* Sirolimus-eluting stents vs paclitaxel-eluting stents in patients with coronary artery disease: meta-analysis of randomized trials. JAMA. 2005;294:819–25.
34. Windecker S, Remondino A, Eberli FR, Jüni P, Räber L, Wenaweser P, *et al.* Sirolimus-eluting and paclitaxel-eluting stents for coronary revascularization. N Engl J Med. 2005;353:653–62.
35. Uchida K, Sasahara M, Morigami N, Hazama F, Kinoshita M. Expression of platelet-derived growth factor B-chain in neointimal smooth muscle cells of balloon injured rabbit femoral arteries. Atherosclerosis. 1996;124:9–23.
36. Li J, Huang SL, Gui GZ. Platelet-derived growth factor stimulated vascular smooth muscle cell proliferation and its molecular mechanism. Acta Pharmacol sin. 2000;21(4):340–4.
37. Ferns GAA, Rains EW, Sprugel KH, Motani AS, Reidy MA, Ross R. Inhibition of neintimal smooth muscle accumulation after angioplasty by an antibody to PDGF. Science. 1991;253:11 29–32.
38. Rensen SSM, Doevendans PAFM, Eys GJJM. Regulation and characteristics of vascular smooth muscle cell phenotypic diversity. Neth Heart J. 2007;15(Number 3).
39. Lamberts RR, Vaessen RJ, Westerhof N, Stienen GJM. Right ventricular hypertrophy causes impairment of left ventricular diastolic function in the rat. Bas Res Cardiol. 2007;102(1):19–27.